Research Square

Preprints are preliminary reports that have not undergone peer review.
They should not be considered conclusive, used to inform clinical practice,
or referenced by the media as validated information.

Chromosome-scale genome assembly of *Verticillium longisporum* CVL1: validation of species-specific genomic fragment VLspe2 and establishment of a one-tube visual RPA-CRISPR/Cas12b detection assay

Yang Chen
State Key Laboratory of Vegetable Biobreeding, Institute of Vegetables and Flowers, Chinese Academy of Agricultural Sciences, Beijing 100081, China

Yuqing Lai
State Key Laboratory of Vegetable Biobreeding, Institute of Vegetables and Flowers, Chinese Academy of Agricultural Sciences, Beijing 100081, China

Kun Qian
State Key Laboratory of Vegetable Biobreeding, Institute of Vegetables and Flowers, Chinese Academy of Agricultural Sciences, Beijing 100081, China

Yuxin Zhang
State Key Laboratory of Vegetable Biobreeding, Institute of Vegetables and Flowers, Chinese Academy of Agricultural Sciences, Beijing 100081, China

Simeng Chang
State Key Laboratory of Vegetable Biobreeding, Institute of Vegetables and Flowers, Chinese Academy of Agricultural Sciences, Beijing 100081, China

Zhenchuan Mao
State Key Laboratory of Vegetable Biobreeding, Institute of Vegetables and Flowers, Chinese Academy of Agricultural Sciences, Beijing 100081, China

Jianlong Zhao
State Key Laboratory of Vegetable Biobreeding, Institute of Vegetables and Flowers, Chinese Academy of Agricultural Sciences, Beijing 100081, China

Guohua Chen
State Key Laboratory of Vegetable Biobreeding, Institute of Vegetables and Flowers, Chinese Academy of Agricultural Sciences, Beijing 100081, China

Jian Ling
lingjian@caas.cn

State Key Laboratory of Vegetable Biobreeding, Institute of Vegetables and Flowers, Chinese Academy of Agricultural Sciences, Beijing 100081, China

---

Research Article

Keywords: Verticillium longisporum, high-quality reference genomes, RPA-CRISPR/Cas12b, one-tube visual detection assay

Posted Date: October 9th, 2026

DOI: https://doi.org/10.21203/rs.3.rs-11139450/v1

License: This work is licensed under a Creative Commons Attribution 4.0 International License. Read Full License

Additional Declarations: No competing interests reported.

Abstract

Background

Verticillium longisporum is a soil-borne hybrid fungal pathogen that causes destructive vascular wilt in oilseed rape and other cruciferous crops, resulting in substantial yield losses. High-quality chromosome-scale genomic resources and detection assays are available for European *V. longisporum* isolates. Several molecular detection assays have been reported for this pathogen in China. However, these assays were built upon genomic data obtained from non-Chinese isolates. Genomic resources originating from indigenous Chinese *V. longisporum* strains remain limited, which hinders precise local disease monitoring and management.

Results

Here, we report the first chromosome-scale genome of the Chinese *V. longisporum* isolate CVL1 from Qinghai Province. The 76.31 Mb genome consists of 16 chromosome-level scaffolds, completely resolving the A1 and D3 subgenomes with 99.2% BUSCO completeness. Using this genomic resource, VLspe2 was validated as a species-specific target sequence that is universally conserved in *V. longisporum* and absent from all closely related *Verticillium* species tested. We further established a one-tube visual detection assay combining RPA and CRISPR/Cas12b. This assay specifically detects as few as 10 copies/μL at about 40°C, produces naked-eye results within 40 min, and requires only a simple constant-temperature device.

Conclusion

This subgenome-resolved chromosome-scale genome of Chinese *V. longisporum* CVL1 fills the genomic resource gap for local isolates. The established RPA-CRISPR/Cas12b visual detection assay exhibits excellent specificity, sensitivity, rapidity and portability in species-level validation, with great application potential for field monitoring and quarantine of *V. longisporum*. This study provides a valuable genomic resource for exploring pathogenic mechanisms and offers a reliable detection assay for precise wilt control, supporting agricultural biosecurity and sustainable cruciferous crop production.

1 Introduction

Verticillium longisporum is a soil-borne fungal phytopathogen that causes destructive *Verticillium* stripe disease in brassicaceous crops [1]. As an allodiploid hybrid fungus, *V. longisporum* is categorized into three genetically distinct lineages (A1D1, A1D2, and A1D3) with divergent geographic distribution patterns and host adaptation traits [2]. This pathogen is widely distributed across Europe, North America, and Asia, and infects a broad spectrum of cruciferous crops, including economically crucial crops such as *Brassica napus*, *B. oleracea*, radish, and Chinese cabbage [1–5].

V. longisporum produces highly resilient microsclerotia, the primary dormant structures that can persist in soil for up to 10 years and serve as the initial inoculum for host infection [6]. Stimulated by root

exudates from susceptible hosts, microsclerotia germinate, and the emergent hyphae directionally elongate toward and penetrate root epidermal cells [2, 7]. Following successful root colonization, the pathogen invades host xylem vessels and proliferates to produce abundant conidia. Massive fungal accumulation physically occludes vascular tissues, obstructing the upward translocation of water and nutrients and ultimately suppressing plant growth and development [8]. At the host senescence stage, the fungus colonizes senescent perivascular tissues and generates new microsclerotia, which return to the soil through plant residue decomposition to complete the disease cycle [9].

Owing to its robust environmental adaptability and persistent soil survival ability, *V. longisporum* has posed escalating threats to global brassica crop production. In addition to traditional epidemic regions in Europe and Canada, frequent disease outbreaks have recently occurred in China, resulting in severe economic losses in local cruciferous crop industries [2, 11, 12]. Field surveys have demonstrated that *B. napus* fields infected with *V. longisporum* typically suffer 10%–50% yield losses [9, 13]. Such expanding prevalence and economic damage underscore the urgent need for sensitive, rapid, and field-applicable diagnostic strategies for precise pathogen monitoring and targeted disease management [14]. While high-quality chromosome-scale genomes are available for European *V. longisporum* isolates, comprehensive genomic resources and portable detection assays remain insufficient for Chinese endemic strains.

Isothermal amplification technologies, including LAMP, RCA, and RPA, have emerged as promising thermocycler-free alternatives for point-of-care (POCT) pathogen detection. Nevertheless, each technique has inherent technical limitations: LAMP relies on complex multiple primer sets and is prone to non-specific amplification and false-positive results [15], whereas RCA requires additional enzymatic treatment and multi-step operational procedures, restricting its on-site application [16]. As a superior isothermal amplification platform, RPA operates steadily at a constant low temperature (37–42°C) with a single primer pair, yet its intrinsic non-specific amplification artifacts frequently induce false-positive signals and compromise detection reliability in non-laboratory environments [17, 18].

CRISPR-Cas systems have been extensively repurposed for nucleic acid diagnostic assays owing to their programmable target recognition and collateral cleavage activity [19]. A diverse panel of Cas effectors, including Cas9, Cas12a, Cas12b, Cas13a, Cas13b and Cas14, have been adapted for nucleic-acid detection [20]. Among these effectors, Cas12b (formerly C2c1), a Class 2 type V-B endonuclease, possesses desirable features for diagnostic applications [21]. Guided by sgRNA, Cas12b specifically recognizes dsDNA targets bearing the canonical 5'-TTN-3' PAM sequence and triggers robust non-specific trans-cleavage of nearby ssDNA reporter probes. Compared with Cas12a, Cas12b has a smaller molecular mass and a broad thermal tolerance range (4°C–100°C), while maintaining high target specificity [23]. This unique thermal adaptability allows Cas12b to function well in isothermal amplification systems with variable reaction temperatures. Notably, the strict sgRNA-target base-pairing dependence of Cas12b trans-cleavage effectively eliminates non-specific amplification artifacts during pre-amplification, greatly improving detection accuracy [24]. Integrating Cas12b with isothermal amplification such as RPA establishes a highly specific POCT platform, which has been successfully

applied for the rapid detection of multiple pathogens, including *Mycoplasma pneumoniae*, *Burkholderia mallei*, *Bactrocera dorsalis* and *Acidovorax citrulli* [24-27].

In this study, we aimed to develop a precise and rapid detection assay for *V. longisporum* based on the RPA-CRISPR-Cas12b system. We constructed a genome assembly for a *V. longisporum* isolate from Qinghai Province by integrating Illumina short-read, PacBio HiFi long-read, and Hi-C chromatin-conformation sequencing data, and performed subgenome assignment to resolve its hybrid-origin subgenomic compartments, which allowed us to evaluate marker conservation at the subgenome level. Using this genomic resource, we reevaluated the previously reported species-specific genomic fragment VLspe2 using rigorous comparative genomic analyses. Our analyses confirmed that VLspe2 is fully conserved in this Chinese isolate, supporting its suitability as a reliable molecular marker. We then designed multiple sets of RPA primers and three sgRNAs targeting VLspe2 and performed screening to identify the optimal primer-sgRNA combination. On this basis, we established a sensitive and specific visual detection assay by integrating the optimized RPA primers and sgRNA into the RPA-CRISPR-Cas12b detection system. This work not only generates a valuable genomic resource for Chinese *V. longisporum* but also provides a new detection assay for this devastating soil-borne fungal pathogen.

2 Methods

2.1 Strains used in this study

V. longisporum strain CVL1 was generously provided by Prof. Jing Zhang's group at Huazhong Agricultural University. *V. longisporum* (DSM12233), *V. dahliae, V. albo-atrum*, and other fungal strains used in this study were deposited at the Institute of Vegetables and Flowers, Chinese Academy of Agricultural Sciences. Detailed information for all strains is summarized in Table 1.

Table 1
Information of tested strains

No.	Species	Source	Location	Detection result
CVL1	*Verticillium longisporum*	Our study	Qinghai, China	+
VL	*Verticillium longisporum*	DSM12233	Germany	+
VA	*Verticillium albo-atrum*	DSM12231	Germany	-
VD1	*Verticillium dahliae*	ACCC 36931	Beijing, China	-
VD2	*Verticillium dahliae*	ACCC 36932	Beijing, China	-
VD3	*Verticillium dahliae*	ACCC 36933	Beijing, China	-
Pu1	*Pythium ultimum*	Our laboratory	Beijing, China	-
phw808	*Fusarium oxysporum*	Our laboratory	Beijing, China	-
PL1	*Polymyxa graminis*	Our laboratory	Beijing, China	-
AL1	*Alternaria solani*	Our laboratory	Beijing, China	-
Note: “+”: positive; “-”: negative				

Table 2
The genome assembly statistics results of *V. longisporum*

Metric	Value
Assembly size(Mb)	76.31
Number of contigs	111
Number of chromosomes	16
N_{50}(Mb)	6.05
GC(%)	52.97
Repeat sequence (Mb)	10.57
Coding sequence	19504
BUSCO completeness(%)	99.20

2.2 Materials

All primers were synthesized by Tsingke Biotechnology (Beijing, China). Sequences of sgRNAs and primers used in this study are listed in Additional file 1, Table S1, S2. The SynSor DNA Isothermal Amplification Kit was purchased from Beijing SynsorBio Technology Co., Ltd. The *pEASY*®-T&B Simple Cloning Kit was obtained from TransGen Biotechnology (Beijing, China).

2.3 Strain collection, cultivation, and genomic DNA extraction

V. longisporum strain CVL1, isolated from Xining, Qinghai, China, was routinely cultured on potato dextrose agar (PDA) at 25°C. For nucleic acid extraction, mycelia were harvested from liquid Czapek-Dox medium grown at 180 rpm, and immediately snap-frozen in liquid nitrogen. High-molecular-weight genomic DNA for high-quality genome analysis of *V. longisporum* was extracted using the CTAB method and further purified with the QIAGEN Genomic DNA Kit. (detailed protocol provided in Supplementary file 1). For RPA-CRISPR/Cas12b detection, template DNA was rapidly prepared via an alkaline lysis (AL) method. Total RNA was isolated with the RNeasy Mini Kit (QIAGEN) to construct RNA-seq libraries.

2.4 Genome sequencing and assembly

A total of 8.75 Gb (~ 115×) Illumina paired-end short reads, 7.00 Gb (~ 97×) PacBio HiFi long reads, and 9.11 Gb (~ 119×) Hi-C chromatin-contact reads were generated for the genome assembly (Table S3). PacBio HiFi long-reads of CVL1 were de-novo assembled with hifiasm (v0.19.5) [28], using a k-mer-derived estimated genome size of 70 Mb from Illumina short reads (Figure S3) [29]. Clean reads of Hi-C sequences were obtained after quality control, which were processed and mapped to the assembled contigs by juicer [30]. Genome error correction and chromosomal-level assembly were then performed via the 3D-DNA pipeline [31], and manual inspection and assembly adjustment were finally conducted using Juicer Box [32]. RNA-seq data were generated to support gene annotation.

2.5 Parental origin determination

To resolve the lineage of the CVL1 strain, average nucleotide identity (ANI) analysis was performed with fastANI. The *V. longisporum* CVL1 genome was aligned against the *V. dahliae* JR2 genome using nucmer (MUMmer-4.0.0-beta2) with the --maxmatch parameter to capture all subgenomic homologous sequences. Alignments were filtered to retain alignment blocks longer than 10 000 bp with ≥ 80% sequence identity and converted into a tab-delimited coordinate table via show-coords with parameters -r -H -T. Subgenome assignment was subsequently conducted using a custom Python script. Valid alignment blocks were sorted by chromosome length and physical position, and each block was assigned to either the A1 or D3 subgenome according to sequence identity thresholds. Adjacent intervals receiving the same subgenome assignment were merged into continuous segments. Regions without reliable mapping evidence were labelled as undefined for conservative classification. For further validation, CDS sequences of CVL1 were queried against JR2 CDS sequences using blastn to examine subtype-specific variations at the coding level. Following subgenome partitioning, BEDTools was used to extract sequences corresponding to the A1 and D3 subgenomes based on the final interval coordinates. BUSCO assessments were run independently on the extracted A1 and D3 subgenomes to quantitatively evaluate the reliability and accuracy of subgenome assignments.

2.6 Genome annotation

This library integrated the Repbase database (v20.05) for homology-based prediction and a de novo repeat library built with MITE-HUNTER, REPEATSCOUT, LTR-FINDER, and PILER-DF [33, 34, 35]. Finally, REPEATMASKER (v 4.0.9) [36] was used to identify and classify the repeats.

Three complementary strategies were applied for protein-coding gene prediction. Homology-based gene prediction was performed using GEMOMA (v1.3) [37]. Ab initio gene prediction was carried out with GENESCAN [38], AUGUSTUS (v2.7) [39], GLIMMERHMM (v3.0.4) [40], GENEID (v1.4) [41], and SNAP [42]. RNA-seq reads of *V. longisporum* were assembled using HISAT2 (v2.0.4) [43] and STRINGTIE (v1.2.3) [44]; the resulting transcripts were processed by PASA (v2.0.2) [45] to identify iso-genes and improve gene-model predictions. Finally, all gene-model evidence was integrated using EVIDENCEMODELER [46].

2.7 Comparative genomics analysis

Whole-genome collinearity between the published high-quality *V. longisporum* reference genome and our newly assembled genome was analyzed using MUMmer 3 [47]. Genome-wide pairwise alignment was performed with nucmer (--maxmatch) to obtain all valid genomic matches. Raw alignments were filtered with delta-filter to keep collinear blocks ≥ 1000 bp and with ≥ 80% nucleotide identity. Filtered collinearity results were visualized via mummerplot to generate high-resolution PNG graphics.

To verify the specificity of the target sequence VLspe2, we performed genome-wide homology searches using blastall against whole-genome datasets of *V. dahliae* and other closely related fungi. Nucleotide databases were built using formatdb (-p F). blastall searches were run with an E-value threshold of 1e-5, and low-complexity filtering was disabled (-F F). Significant homologous hits were defined by E-value ≤1e-5, query coverage ≥ 100 bp, and sequence identity ≥ 70%.

2.8 Detection target

VLspe2, a species-specific genomic fragment, was used as the target sequence of this RPA-CRISPR/Cas12b detection assay (GenBank index numbers: JAETXT010000013.1, 1634227–1635226). Using genomic DNA of *V. longisporum* as template, the target fragment was amplified with primers VL-PCR-F and VL-PCR-R. The PCR product was ligated into the pEASY-T&B Simple Cloning vector to generate recombinant plasmid standards for subsequent detection experiments.

2.9 sgRNA design and validation

Candidate target regions were selected from documented loci, with host-homologous sequences discarded. sgRNAs were filtered and assigned composite scores based on PAM position, GC content, intramolecular dimerization, target accessibility, base-position preference and predicted off-target specificity. Normally, three top-ranked candidates with composite scores > 40 were retained. Additional candidates were included when few candidates met this score cutoff and satisfied all filtering criteria. Spacer sequences that may disrupt the secondary structure of the vector backbone were excluded to preserve assay specificity and sensitivity.

PCR primers were designed to cover 100 bp flanking sequences on each side of the sgRNA target site, and the resulting amplicons were used as validation templates. The 50 μL AaCas12b reaction system contained 2 μL of 2.5 μM SynSor AaCas12b, 1 μL of 100 ng/μL SynSor sgRNA, 5 μL of 10× reaction buffer, 0.5 μL of 100 μM 12b-FAM ssDNA reporter, 1 μL of DNA template, and nuclease-free water to the final volume. The reaction was incubated at 43°C for 15 min on SLAN-96P real-time PCR system (Shanghai Hongshi Medical Technology Co., Ltd., China), with FAM fluorescence recorded at 1-minute intervals. sgRNA performance and specificity were evaluated using fluorescence kinetic curves, where effective candidates showed a clear plateau of fluorescence signal between target samples and negative controls. The fluorescence growth rate (Fluorescence Slope) was calculated as: Fluorescence Slope = (R_n - R_1)/R_1, where R_n is the fluorescence signal at minute n, and R_1 is the fluorescence signal of the negative control at the first minute.

2.10 RPA primer design and validation

Candidate RPA primers (30–35 nt) were selected within the target region. To ensure robust and specific amplification, primer GC content was set between 40% and 60%, and expected amplicons ranged from 100 to 200 bp. Three forward and three reverse primers were designed, and NCBI Primer-BLAST was used to assess amplification coverage and specificity. Serially diluted plasmids (10^4 copies/μL and 10^3 copies/μL) were utilized to screen primer combinations using one-tube RPA-CRISPR/Cas12b reactions.

2.11 Establishment of the one-tube RPA-CRISPR/Cas12b detection assay

The RPA-CRISPR/Cas12b assay adopts a tube-cap pre-loading strategy to physically separate RPA and CRISPR-Cas12b components before reaction. The 20 μL RPA mixture was prepared by resuspending the lyophilized pellet in 12 μL rehydration buffer, then supplemented with 1 μL MgOAc (280 mM), 2 μL forward primer (10 μM), 2 μL reverse primer (10 μM), 2 μL template, and 1 μL nuclease-free ddH_2O. Tubes were capped and briefly centrifuged. The 10 μL CRISPR-Cas12b mixture, containing 1 μL AaCas12b (50 ng/μL), 0.5 μL sgRNA (250 ng/μL), 0.33 μL 12b-FAM ssDNA Reporter (100 μM), 1 μL 10× AaCas12b Buffer and 7.17 μL nuclease-free ddH_2O, was loaded onto tube caps above the RPA solution without centrifugation. Tubes were incubated at 42°C for 15 min in a conventional water-bath for RPA amplification. Brief centrifugation combined amplicons with the CRISPR mixture to initiate Cas12b-mediated cleavage, followed by a further 30 min incubation at 42°C. For assay performance characterization in this study, kinetic fluorescence signals were collected using the SLAN-96P real-time PCR system, with recordings taken every minute. After incubation, tubes were illuminated with a 485 nm blue-LED lamp for naked-eye result interpretation based on visible color changes. For qualitative naked-eye detection, all incubation steps could be completed with a conventional water-bath without fluorescence-recording equipment.

2.12 Specificity and Sensitivity Evaluation of the RPA-CRISPR/Cas12b assay

Assay specificity was evaluated using genomic DNA extracted from *V. longisporum*, *V. dahliae*, *V. albo-atrum* and other fungal strains. The recombinant plasmid carrying the VLspe2 fragment served as the positive control, and sterile water served as the negative control. Preliminary sensitivity assays were carried out using 10-fold serially diluted VLspe2 plasmid. To further characterize detection performance, additional replicates were tested at the limit of detection (10 copies/μL) and adjacent concentration (50 copies/μL).

3 Result

3.1 High-quality chromosome-scale genome assembly and structural profiling of *V. longisporum* CVL1

A chromosome-scale genome assembly was generated for *V. longisporum* isolate CVL1.The final assembly contained 111 contigs, with a total size of 76.31 Mb and a contig N50 of 6.06 Mb (Fig. 1A). Using Hi-C data, 76.31 Mb of sequences were clustered into 16 chromosomes. The slight difference between the assembled genome and the k-mer-estimated genome size (~ 70 Mb) is probably caused by more repetitive sequences recovered in the CVL1 genome (Additional file 1: Figure S1). Further evaluation, using BUSCO (v5.4.0), indicated that 99.20% of conserved orthologs were fully captured by the CVL1 assembly (Additional file 1: Table S3). For structural validation of the chromosome-level assembly, whole-genome collinearity analysis was performed against reference strain PD589. Strong global synteny was observed, with only minor local disruptions and no large-scale chromosomal rearrangements, confirming high structural fidelity of our assembly (Additional file 1: Figure S2).

To clarify the hybrid lineage of CVL1, average nucleotide identity (ANI) analysis was implemented using FastANI. The high genome-wide ANI value of 99.92% between CVL1 and the well-characterized A1/D3 lineage reference strain PD589 confirmed that CVL1 belongs to the A1/D3 hybrid lineage of *V. longisporum* (Additional file 1: Table S4). Resolving the parental origin of subgenomes origin is critical for characterizing the genomic architecture of hybrid-origin *V. longisporum*. Given that the D3 parent of hybrid-origin *V. longisporum* is phylogenetically more closely related to *V. dahliae* than the A1 parent [2], whole-genome alignment between CVL1 and *V. dahliae* exhibited a distinct bimodal sequence identity distribution (Additional file1: Figure S5). Based on this unique bimodal divergence feature combined with subgenome integrity evaluation, we defined a rigorous three-tier threshold set for accurate subgenome partitioning: genomic regions with sequence identity < 96.0% were assigned to the A1 subgenome, regions with identity > 96.5% were assigned to the D3 subgenome, and regions with identity ranging from 96.0% to 96.5% were defined as ambiguous regions that could not be accurately assigned to either subgenome. Independent coding sequence alignment further verified this bimodal divergence feature, confirming the robustness of the subgenome classification strategy. Following this standardized threshold, a total of 36 Mb of sequences were successfully anchored to the A1 subgenome with a BUSCO completeness of 97% (Additional file 1: Table S6, S7), and 34.2 Mb of sequences were classified into the D3 subgenome with a BUSCO completeness of 98% (Additional file 1: Table S7, S8). A total of

6.32 Mb genomic sequences (8.3% of the total assembly) could not be confidently attributed to either parental origin or were designated as ambiguous regions. The two partitioned subgenomes exhibited balanced and reasonable sizes and high integrity, consistent with the typical haploid genome scale of *Verticillium* species. Notably, Circos visualization of full-length chromosomes revealed an obvious mosaic genomic pattern, a typical biological characteristic of hybrid-derived *V. longisporum*, which clearly presented the interspersed distribution of A1 and D3 subgenomic fragments across 16 chromosomes (Fig. 1B).

3.2 Multi-level genomic annotation of *V. longisporum* genome (CVL1)

Repetitive sequences constituted 13.86% (10, 574,683 bp) of the genome, dominated by transposable elements where LTR retrotransposons were the major component (Additional file1: Table S9, S10). Non-LTR retrotransposons (LINE/SINE) and tandem repeats occurred at low abundance. Following repeat masking, 19 504 protein-coding genes were predicted (Additional file1: Table S11). Among non-coding RNAs, 18S rRNA was the most abundant, comprising 2.24% of the genome; complete ncRNA statistics are listed in Additional file1, Table S12. Overall, 99.8% of predicted protein-coding genes obtained functional annotations from the NR, GO, COG, and KEGG databases. Enrichment analysis revealed over-representation of genes associated with central carbon metabolism, genetic regulation, and pathogen-host interaction pathways (Additional file 1: Figure S4-S6).

3.3 Conservation verification of the specific target fragment VLspe2 based on sequence alignment

The species-specific fragment VLspe2 (1001 bp), identified in our earlier work, was selected as the candidate target for the RPA-CRISPR/Cas12b assay. High genomic similarity exists among *V. longisporum, V. dahliae*, *V. alfalfae* and *V. nonalfalfae*. Previously published data demonstrated full-length 100% sequence identity of VLspe2 across eight *V. longisporum* genomes (Additional file 1: Table S13). VLspe2 was further aligned against our CVL1 chromosome-scale assembly and reference genomes of these three closely related *Verticillium* species. Taken together, CVL1 exhibited full-length 100% identity, whereas no full-length homologous hits were detected in related species. Copy-number assessment confirmed VLspe2 as a single-copy fragment located on Chr 16 (positions 400 847–401 847) belonging to the A1 subgenome of the CVL1 genome (Fig. 1B; Additional file 1: Table S14). Thus, VLspe2 is a suitable target sequence for the RPA-CRISPR/Cas12b assay.

3.4 Optimization of core components for the RPA-CRISPR/Cas12b visual detection assay

Owing to its confirmed species-specificity and high intra-species conservation, the VLspe2 fragment was chosen as the target sequence to develop an RPA-CRISPR/Cas12b visual detection assay. Three sgRNAs, together with three forward and three reverse RPA primers, were rationally designed to target

distinct regions of VLspe2. Cross-combination of these forward and reverse primers generated nine RPA primer pairs with mutually non-overlapping binding sites.

All sgRNA screening was performed using recombinant plasmids carrying VLspe2. To avoid interference between RPA amplification and Cas12b cleavage, sgRNA performance was quantified in a standalone CRISPR-Cas12b system according to maximum fluorescence intensity and 15-min signal accumulation rate. sgRNA3 produced markedly stronger fluorescence with faster signal saturation. Owing to its excellent target-binding and trans-cleavage activity, it was selected as the optimal sgRNA for the integrated detection system (Fig. 2A-B).

With sgRNA3 fixed, all nine primer pairs were further screened using the same VLspe2 recombinant plasmids at template doses of 1×10^3 and 1×10^4copies, by comparing fluorescence profiles and signal-generation kinetics. Most primer pairs exhibited obvious signal attenuation at low template abundance, while VL-RPA-F2/R3 yielded stable intense signals under both concentrations (Fig. 3A-C), demonstrating balanced amplification efficiency and robust sensitivity across varying pathogen loads. Collectively, sgRNA3 and VL-RPA-F2/R3 were confirmed as the optimal matching core components, laying a solid foundation for subsequent performance validation of the detection assay.

3.5 Specificity of the RPA-CRISPR/Cas12b visual detection assay

The RPA-CRISPR/Cas12b assay generated intense fluorescence signals exclusively for two *V. longisporum* strains: CVL1 (isolated in this study) and reference strain DSM 12233. No detectable signals were observed for closely-related *Verticillium* species (*V. dahliae*, *V. albo-atrum*) or negative controls, confirming an absence of cross-reactivity against non-target templates (Fig. 4A, B). To further verify the performance of this detection assay, parallel blue-light visual detection corroborated quantitative fluorescence readouts, yielding highly consistent results across the two detection modes (Fig. 4C). Collectively, these results demonstrate that the assay enables specific discrimination of *V. longisporum* from close-related *Verticillium* pathogens using the VLspe2 sequence.

3.6 Sensitivity of the RPA-CRISPR/Cas12b visual detection assay

We serially diluted target pathogen nucleic acids to systematically characterize the analytical sensitivity of our RPA-CRISPR/Cas12b visual detection assay, ranging from 10^5 copies/μL to 1 copy/μL (Fig. 5). Serially diluted templates were analyzed using real-time fluorescence kinetic quantification and blue-light visual detection in parallel with biological replicates. Fluorescence kinetic profiling preliminarily defined the assay LOD as 10 copies/μL, and consistent distinct visual signals were reliably observed at this concentration across all replicate tests. The stable and identifiable fluorescent signals at both 10 copies/μL (preliminary LOD) and 50 copies/μL (higher concentration) validated the excellent practicability and stability of this dual-mode system for low-abundance template detection. Collectively,

the definitive LOD of this RPA-CRISPR/Cas12b diagnostic assay was determined to be 10 copies/μL (Fig. 6).

4 Discussion

High-quality reference genomes are critical for understanding the evolutionary dynamics of hybrid-origin *Verticillium* species and identifying species-specific DNA sequences for pathogen diagnostics [2]. Previous morphological methods, PCR, and qPCR approaches all have their respective limitations. In this study, we generated a high-quality chromosome-scale assembly of *V. longisporum* isolate CVL1 and resolved its two parental subgenomes using a three-tier partitioning strategy. Leveraging this improved genomic resource, we validated the species-specific marker VLspe2 and developed a one-tube visual RPA-CRISPR/Cas12b assay for rapid detection of *V. longisporum*.

Compared with the previously published PD589 assembly, our CVL1 assembly avoids the disassembly of highly repetitive regions observed in PD589[48]. The PD589 assembly exhibited one chromosome with abnormally strong Hi-C interactions and approximately two-fold higher read coverage than other chromosomes, indicative of collapsed duplications and a probable total of 17 chromosomes. Our CVL1 genome contains none of these assembly-related errors and offers a more reliable basis for precise subgenome assignment. Using this improved assembly, we adopted a three-tier partitioning strategy to reduce the binary assignment bias present in previous subgenome classification approaches. We set a specific similarity range for ambiguous sequences, so recombinant regions remained unassigned rather than being randomly grouped into one of the two parental subgenomes [48]. This strategy produced well-balanced A1 and D3 subgenomes and clearly recovered a set of ambiguous sequences, which may partly reflect genetic signatures of post-hybridization recombination.

The well-resolved genomic resource also enabled precise mapping of the species-specific fragment VLspe2 to the A1 subgenome, providing a foundation for the RPA-CRISPR/Cas12b detection assay. In the earlier study, we identified VLspe2 as a *V. longisporum*-specific fragment, verified its intra-species conservation and inter-species specificity, and developed an EmDEA isothermal detection assay based on this target sequence [49]. However, no chromosome-scale assembly was available for Chinese isolates at that stage, leaving the subgenomic origin and copy number of VLspe2 uncharacterized. Using the present assembly, we confirmed that VLspe2 is a single-copy element confined to the A1 subgenome. Further alignment of this region to reference genomes of closely related *Verticillium* species provided additional genomic-level support for its specificity.

Supported by these genomic validations, we characterized the performance of the RPA-CRISPR/Cas12b detection assay. The optimized assay showed high species specificity, with no cross-reactions against closely related fungal pathogens. With a limit of detection of 10 copies per reaction within 40 minutes, the system allows direct visual readout under blue-light illumination and does not require fluorescence quantification equipment [50]. Although the previously reported EmDEA assay also targets VLspe2 and achieves high sensitivity, its signal readout depends on dedicated fluorescence-detecting instruments.

Compared with the EmDEA assay, the one-tube visual RPA-CRISPR/Cas12b assay has a broader applicability and is better suited for field screening and quarantine inspection at ports.

Despite these improvements, this study has two main limitations. First, genomic analyses and subgenome assignment were based on a single *V. longisporum* isolate. Larger global strain collections covering diverse hybrid lineages and field isolates are required to validate the generalizability of our findings and three-tier strategy. Second, our RPA-CRISPR/Cas12b assay was only validated using purified DNA from cultured isolates; its real-world stability and detection accuracy remain untested on naturally infected plant tissues and infested field soil samples [51].

5. Conclusion

In this study, we generated a high-quality chromosome-scale genome assembly of *V. longisporum* isolate CVL1 and performed subgenome assignment using a three-tier strategy to mitigate binary-assignment bias for hybrid-origin fungal pathogens. This improved genomic resource enabled unambiguous mapping of the species-specific fragment VLspe2 to the A1 subgenome and confirmed its single-copy status. Building on these genomic validations, we established a one-tube visual RPA-CRISPR/Cas12b assay for rapid detection of *V. longisporum*. The assay exhibits high species-specificity and low limit of detection and supports direct blue-light visual readout without specialized equipment, showing great potential for field screening and port quarantine. Our study demonstrated the value of high-resolution chromosome-scale assemblies for studying hybrid fungal pathogens and provides a practical molecular diagnostic assay for *V. longisporum*. Future work should address these gaps to facilitate practical deployment of this molecular diagnostic assay.

Declarations

Acknowledgements

We would like to extend our sincere gratitude to all colleagues involved in this work. We highly appreciate their insightful discussions, valuable comments, and diligent technical assistance, which were of great significance for promoting this research and polishing the manuscript.

Author contributions

G.C. and J.L. conceived and designed the research and supervised the whole study. Y.C., Z.C.M., Y.Q.L., K.Q., Y.X.Z. and S.M.C. performed experiments, data collection and formal data analysis (Investigation, Data curation, Formal analysis). Y.H.Y. contributed experimental materials and revised the manuscript. J.L.Z. participated in experimental design, reviewed and revised the manuscript. Y.C. and J.L. wrote the original draft of the manuscript and completed all subsequent manuscript revisions. All authors have read and approved the final version of the manuscript.

Funding

This research is funded by the National Key R&D Program of China (2023YFC2604900), Key Research and Development Program of Shaanxi (2021ZDLNY05-01), and the National Natural Science Foundation of China (grant numbers: 31571962, 32372508), China Agriculture Research System (CARS-23).

Data availability

The raw sequencing reads (Illumina short-read, PacBio HiFi long-read, and Hi-C) generated for *V. longisporum* have been deposited in the Genome Sequence Archive (GSA) of the National Genomics Data Center (NGDC, https://ngdc.cncb.ac.cn/), under BioProject accession PRJCA032832 and GSA accession CRA045101. The chromosome-scale genome assembly and gene annotation file are available in the Genome Warehouse (GWH) under the same BioProject PRJCA032832, with GWH accession GWHJXXV00000000.1. The A1 and D3 subgenome sequences, all gene CDS sequences and corresponding protein (PEP) sequences of *V. longisporum* were deposited in OMIX (Open Archive for Miscellaneous Data) of NGDC under accession OMIX020908, associated with BioProject PRJCA032832. All datasets are publicly accessible upon publication.

Ethics approval and consent to participate

Not applicable.

Consent for publication

Not applicable.

Competing interests

The authors declare no conflicts of interest related to this work

References

1. Si W, Wang R, Wu M, et al. Identification and virulence test of a new pathogen that causes Verticillium striping on rapeseed in northwestern China. Oil Crop Sci. 2024;9:8–19.
2. Depotter JRL, Deketelaere S, Inderbitzin P, et al. Verticillium longisporum, the invisible threat to oilseed rape and other brassicaceous plant hosts. Mol Plant Pathol. 2016;17:1004–16. 10.1111/mpp.12350.
3. Duan WJ, Li XL, Lü Y, Zhang XM. Development of TaqMan–MGB fluorescent real–time PCR assay for the detection of Verticillium longisporum. Plant Prot. 2023;49:224–32.
4. Tran VT, Braus–Stromeyer SA, Timpner C, Braus GH. Molecular diagnosis to discriminate pathogen and apathogen species of the hybrid Verticillium longisporum on the oilseed crop Brassica napus. Appl Microbiol Biotechnol. 2013;97:4467–83. 10.1007/s00253-012-4530-1.
5. Tyvaert L, França S, Debode J, Höfte M. The endophyte Verticillium Vt305 protects cauliflower against Verticillium wilt. J Appl Microbiol. 2014;116:1563–71. 10.1111/jam.12481.

6. Rafiei V, Dixelius C, Tzelepis G. The soilborne fungus Verticillium longisporum and its interactions with the brassicaceous hosts. Mol. Plant–Microbe Interact. 2025;38:497–504.
7. Zhou L, Hu Q, Johansson A, Dixelius C. Verticillium longisporum and V. dahliae: infection and disease in Brassica napus. Plant Pathol. 2006;55:137–44.
8. Eynck C, Koopmann B, von Tiedemann A. Identification of Brassica accessions with enhanced resistance to Verticillium longisporum under controlled and field conditions. J Plant Dis Prot. 2009;116:63–72.
9. Heale JB, Karapapa VK. The verticillium threat to Canada's major oilseed crop: canola. Can J Plant Pathol. 1999;21:1–7.
10. Dunker S, Keunecke H, von Tiedemann A. Impact of Verticillium longisporum on yield and morphology of winter oilseed rape (Brassica napus) in relation to systemic spread in the plant. J Phytopathol. 2008;156:698–707.
11. Zheng X, Lopisso D, Eseola A, Koopmann B, von Tiedemann A. Potential for seed transmission of Verticillium longisporum in oilseed rape (Brassica napus). Plant Dis. 2019;103:1843–9.
12. Cui J, Strelkov SE, Hwang S–F. Quantifying yield losses in canola (Brassica napus) caused by Verticillium longisporum. Horticulturae. 2025;11:494.
13. Wang Y, Strelkov SE, Hwang S–F. Blackleg yield losses and interactions with Verticillium stripe in canola (Brassica napus) in Canada. Plants. 2023;12:434.
14. Martinelli F, Scalenghe R, Davino S, Panno S, Scuderi G, Ruisi P, Villa P, Stroppiana D, Boschetti M, Goulart LR, Davis CE, Dandekar AM. Advanced methods of plant disease detection. A review. Agron Sustain Dev. 2015;35:1–25.
15. Kim S–H, Lee S–Y, Kim U, Oh S–W. Diverse methods of reducing and confirming false–positive results of loop–mediated isothermal amplification assays: A review. Anal Chim Acta. 2023;1280:341693.
16. Wu X, Yu Z, Guo C, Liu C, Zhang Q, Chen Y, Liu Y, Zhang X. RatioCRISPR: A ratiometric biochip based on CRISPR/Cas12a for automated and multiplexed detection of heteroplasmic SNPs in mitochondrial DNA. Biosens Bioelectron. 2023;241:115670.
17. Daher RK, Stewart G, Boissinot M. Influence of sequence mismatches on the specificity of recombinase polymerase amplification technology. Mol Cell Probes. 2015;29:116–21.
18. Munawar M. Critical insight into recombinase polymerase amplification technology. Expert Rev Mol Diagn. 2022;22:725–37.
19. Cheng X, Li Y, Kou J, Liao D, Zhang W, Yin L, Man S, Ma L. Novel non–nucleic acid targets detection strategies based on CRISPR/Cas toolboxes: a review. Biosens Bioelectron. 2022;215:114559.
20. Zhou J, Li Z, Olajide JS, Wang G. CRISPR/Cas–based nucleic acid detection strategies: Trends and challenges. Heliyon. 2024;10(4):e26179.
21. Li L, Li S, Wu N, Wu J, Wang G, Zhao G, Wang J. HOLMESv2: A CRISPR–Cas12b–assisted platform for nucleic acid detection and DNA methylation quantitation. ACS Synth Biol. 2019;8:2228–37.

22. Teng F, Cui T, Feng C, Guo L, Xu K, Gao Q, Zhou Q, Li W, CDetection. CRISPR–Cas12b–based DNA detection with sub–attomolar sensitivity and single–base specificity. Genome Biol. 2019;20:132.
23. Wang J, Ye X, Liu Y, Li W, Zhang X, Zhang W, Yi C, Liu C. Regulating cleavage activity and enabling microRNA detection with split sgRNA in Cas12b. Nat Commun. 2025;16(1):6427.
24. Feng J, Wu Z, Zhu W, Jin F, Zhao M, Zhong W, Dai C, He Y, Yan L, Wu S, Wang Y, Rui Y, Zheng L, Fu Q. A novel thermo–activated one–pot RPA–CRISPR–Cas12b assay for Mycoplasma pneumoniae POCT. Biosens Bioelectron. 2025;288:117839.
25. Zhang Y, Guo C, Wang H, et al. Construction of an RPA-CRISPR visualization system for rapid detection of Burkholderia mallei. BMC Microbiol. 2026;26:217.
26. Lv C, Zhang F, Wang Y, Li Y, Sun Y, Wang H, Liu B. Rapid visual detection assay for Bactrocera dorsalis (Hendel) using recombinase polymerase amplification and CRISPR/Cas12b. Sci Rep. 2025;15(1):16528.
27. Yang L, Chen G, Wu J, Wei W, Peng C, Ding L, Chen X, Xu X, Wang X, Xu J. A PAM–Free One–Step Asymmetric RPA and CRISPR/Cas12b Combined Assay (OAR–CRISPR) for Rapid and Ultrasensitive DNA Detection. Anal Chem. 2024;96(13):5471–7.
28. Cheng H, Concepcion GT, Feng X, Zhang H, Li H. Haplotype–resolved de novo assembly using phased assembly graphs with hifiasm. Nat Methods. 2021;18(2):170–5.
29. Ranallo–Benavidez TR, Jaron KS, Schatz MC. GenomeScope 2.0 and Smudgeplot for reference–free profiling of polyploid genomes. Nat Commun. 2020;11(1):4325.
30. Durand NC, Robinson JT, Shamim MS, Machol I, Mesirov JP, Lander ES, Aiden EL. Juicebox provides a visualization system for Hi-C contact maps with unlimited zoom. Cell Syst. 2016;3(2):99–101.
31. Dudchenko O, Batra SS, Omer AD, Nyquist SK, Hoeger M, Durand NC, Shamim MS, et al. De novo assembly of the Aedes aegypti genome using Hi-C yields chromosome-length scaffolds. Science. 2017;356(6333):92–5.
32. Durand NC, Shamim MS, Machol I, Rao SSP, Huntley MH, Lander ES, Aiden EL. Juicer provides a one-click system for analyzing loop-resolution Hi-C experiments. Cell Syst. 2016;3(2):95–8.
33. Han Y, Wessler SR. MITE–Hunter: A program for discovering miniature inverted–repeat transposable elements from genomic sequences. Nucleic Acids Res. 2010;38:e199.
34. Price AL, Jones NC, Pevzner PA. De novo identification of repeat families in large genomes. Bioinformatics. 2005;21:i351–8.
35. Edgar RC, Myers EW. PILER: Identification and classification of genomic repeats. Bioinformatics. 2005;21:i152–8.
36. Tarailo–Graovac M, Chen N. Using Repeat Masker to identify repetitive elements in genomic sequences. Curr Protoc Bioinf. 2009;25. 4.10.1-4.10.14.
37. Keilwagen J, Wenk M, Erickson JL, Schattat MH, Grau J, Hartung F. Using intron position conservation for homology–based gene prediction. Nucleic Acids Res. 2016;44:e89.

38. Burge C, Karlin S. Prediction of complete gene structures in human genomic DNA. J Mol Biol. 1997;268:78–94. https://doi.org/10.1006/jmbi.1997.0951.
39. Stanke M, Waack S. Gene prediction with a hidden Markov model and a new intron submodel. Bioinformatics. 2003;19:ii215–25.
40. Majoros WH, Pertea M, Salzberg SL, TigrScan, Glimmer HMM. Two open-source ab initio eukaryotic gene–finders. Bioinformatics. 2004;20:2878–9.
41. Blanco E, Parra G, Guigó R. Using geneid to identify genes. Curr Protoc Bioinf. 2007;18: Unit 4.3.
42. Korf I. Gene finding in novel genomes. BMC Bioinformatics. 2004;5:59. https://doi.org/10.1186/1471-2105-5.
43. Kim D, Langmead B, Salzberg SL. HISAT: A fast spliced aligner with low memory requirements. Nat Methods. 2015;12:357–60. https://doi.org/10.1038/nmeth.3317.
44. Pertea M, Pertea GM, Antonescu CM, Chang TC, Mendell JT, Salzberg SL. StringTie enables improved reconstruction of a transcriptome from RNA–seq reads. Nat Biotechnol. 2015;33:290–5. https://doi.org/10.1038/nbt.3122.
45. Pertea M, Pertea GM, Antonescu CM, Chang TC, Mendell JT, Salzberg SL. StringTie enables improved reconstruction of a transcriptome from RNA–seq reads. Nat Biotechnol. 2015;33:290–5.
46. Haas BJ, Salzberg SL, Zhu W, Pertea M, Allen JE, Orvis J, White O, Buell CR, Wortman JR. Automated eukaryotic gene structure annotation using Evidence Modeler and the Program to Assemble Spliced Alignments. Genome Biol. 2008;9:R7.
47. Kurtz S, Phillippy A, Delcher AL, Smoot M, Shumway M, Antonescu C, Salzberg SL. Versatile and open software for comparing large genomes. Genome Biol. 2004;5:R12.
48. Depotter JRL, van Beveren F, Rodriguez–Moreno L, Kramer HM, Chavarro Carrero EA, Fiorin GL, van den Berg GCM, Wood TA, Thomma BPHJ, Seidl MF. The interspecific fungal hybrid Verticillium longisporum displays subgenome–specific gene expression. mBio. 2021;12(4):e01496–21.
49. Chen Y, Lu X, Mao Z, Li Y, Zhao J, Yang Y, Chen G, Ling J. Rapid detection of the plant pathogenic fungi Verticillium longisporum using species–specific fragment and enzyme mediated duplex exponential amplification (EmDEA) assay. World J Microbiol Biotechnol. 2026;42:178.
50. Lv C, Zhang F, Wang Y, Li Y, Sun Y, Wang H, Liu B. Rapid visual detection assay for *Bactrocera dorsalis* (Hendel) using recombinase polymerase amplification and CRISPR/Cas12b. Sci Rep. 2025;15(1):16528.
51. Wang J, Jiao X, Jia Y, Jin D, Wang Y, Gao Y, Su X. Detection and quantification of *Verticillium dahliae* and *Verticillium longisporum* by droplet digital PCR versus quantitative real–time PCR. Front Cell Infect Microbiol. 2022;12:944156.

Figures

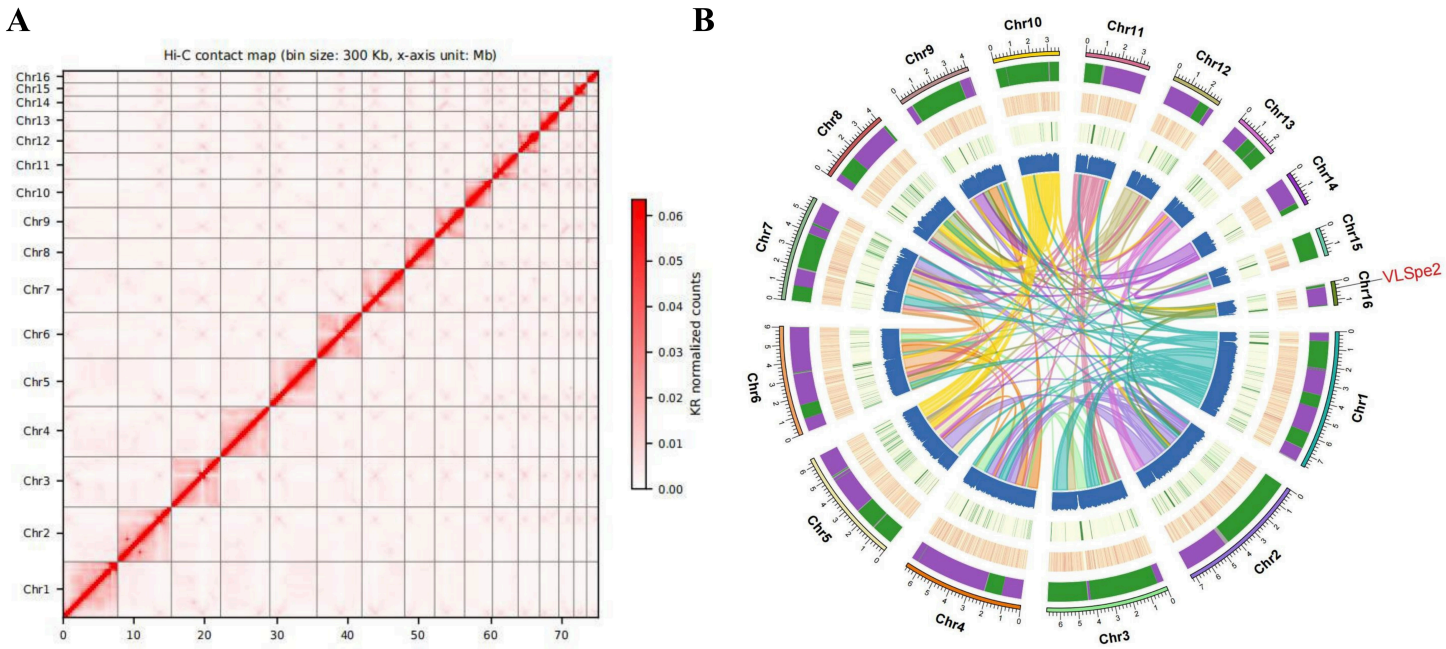


Figure 1

Chromosome-scale assembly validation and genomic-feature circos plot of *V. longisporum* CVL1.

(A) Hi-C contact map (bin size = 300 Kb, KR-normalized; x-axis unit: Mb). Distinct diagonal interactions support reliable chromosome anchoring. (B) Circos visualization of 16 chromosomes. Outer rings show chromosomes and subgenome assignments: A1 subgenome (purple), D3 subgenome (green), undefined ambiguous regions (grey). Inner-to-outer bar charts: syntenic gene blocks from MCScanX, GC content (blue), repetitive-sequence density (green), gene density (orange). Intra-genome syntenic links are shown in multicolor lines. Red label indicates the genomic position of this fragment VLspe2 on Chr16.

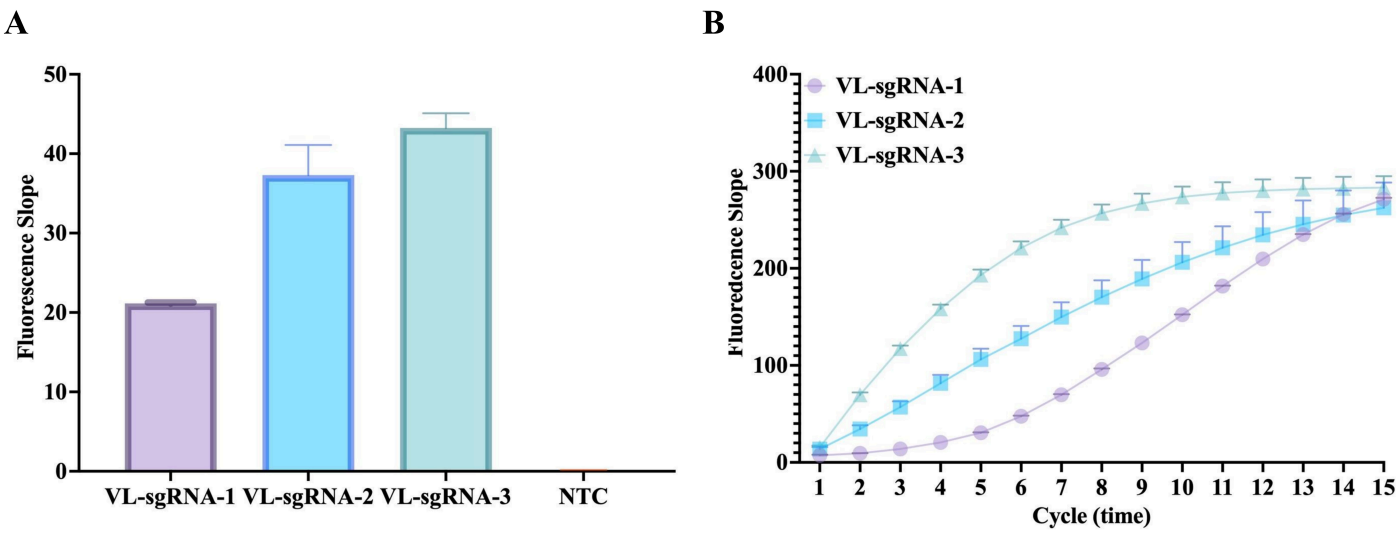


Figure 2

Screening of candidate sgRNAs for RPA-CRISPR/Cas12b detection. (A) Fluorescence slope of three sgRNA candidates. NTC, no-template control. Values are mean ± SD.(B) Real-time fluorescence kinetic curves for VL-sgRNA-1, VL-sgRNA-2 and VL-sgRNA-3 over reaction cycles. VL-sgRNA-3 showed the strongest cleavage-triggered fluorescence signal.

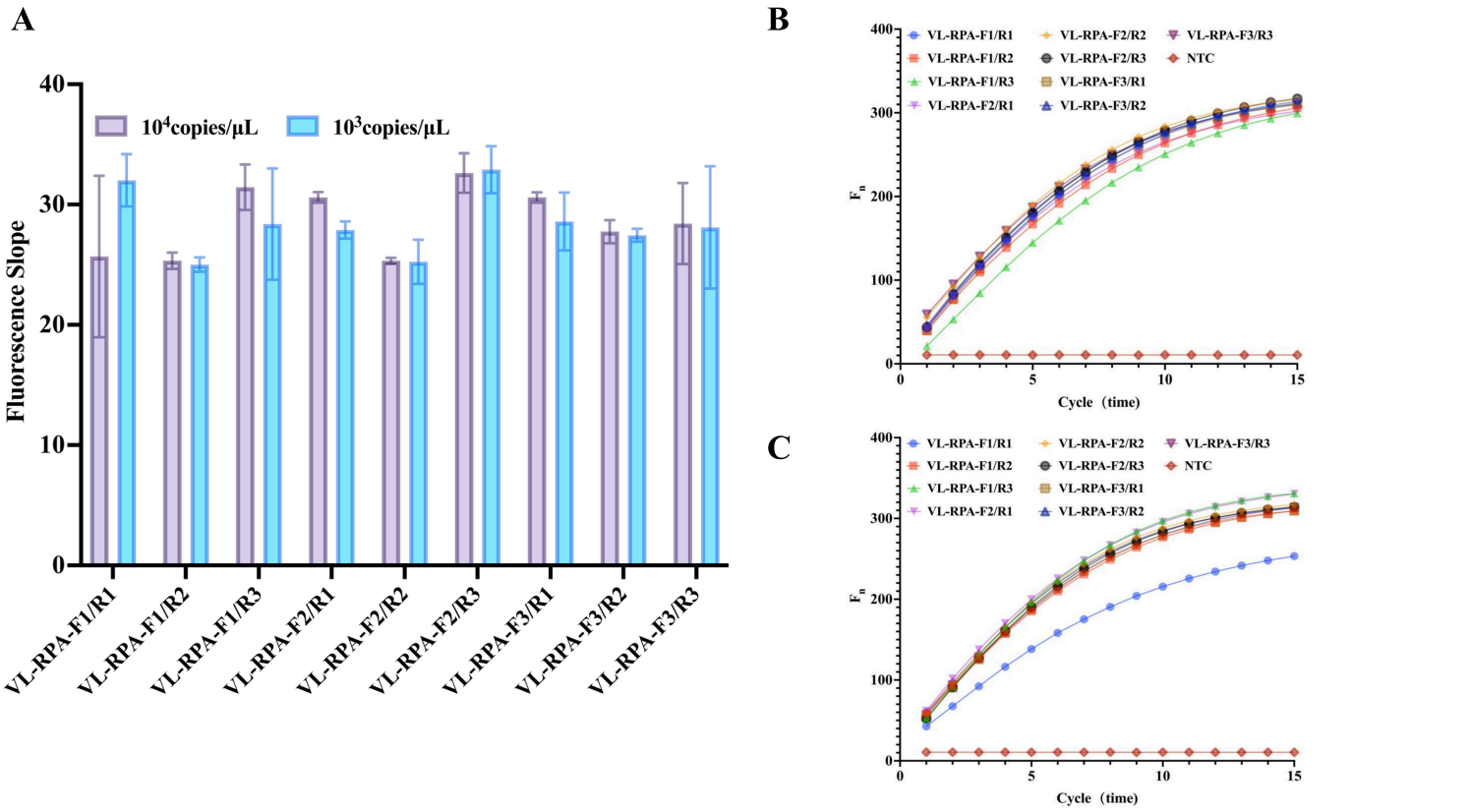


Figure 3

Screening of RPA primer combinations for the RPA-CRISPR/Cas12b detection system.(A) Fluorescence slope values of nine RPA primer pairs at two template concentrations (10^4 and 10^3 copies μL^{-1}). Data represent mean ±SD.(B) Real-time fluorescence kinetic curves for nine primer combinations under high-concentration template. NTC, no-template control.(C) Real-time fluorescence kinetic curves for nine primer combinations under low-concentration template. NTC, no-template control.

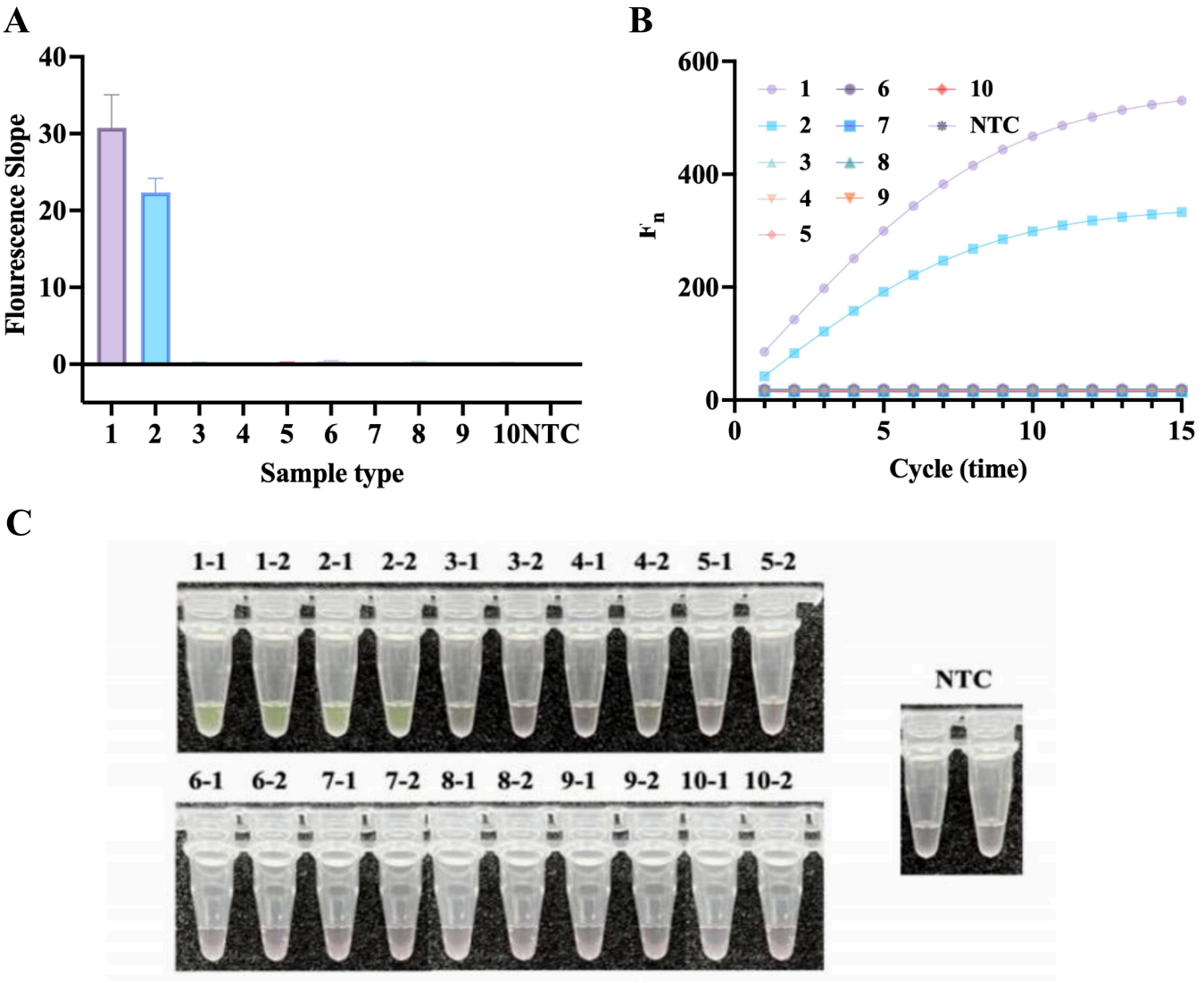


Figure 4

Performance of the one-tube visual RPA-CRISPR/Cas12b detection assay (A) Fluorescence change rate for different DNA samples. Data represent mean ± SD. (B) Real-time fluorescence curves of different DNA samples.(C) Visual readout of the assay in reaction tubes.Samples 1-2: *Verticillium longisporum* (1, isolate CVL1; 2, DSM12233); 3-5: *Verticillium dahliae*; 6: *Pythium ultimum*; 7: *Fusarium oxysporum*; 8: *Verticillium albo-atrum*; 9: *Polymyxa graminis*; 10: *Alternaria solani*. NTC, no-template control. Positive reactions exhibit visible green fluorescence, whereas negative samples remain colourless.

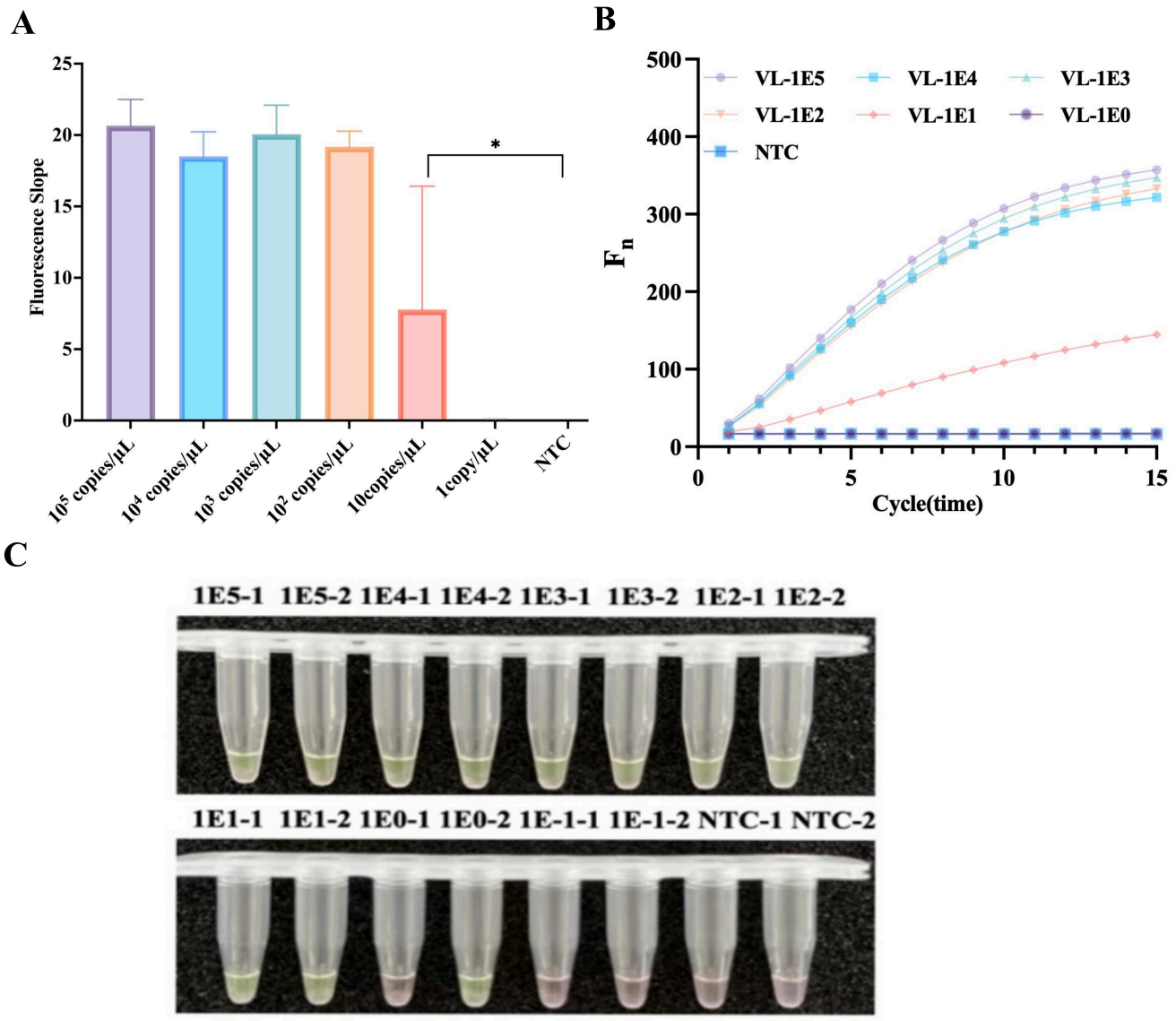


Figure 5

Sensitivity evaluation of the one-tube visual RPA-CRISPR/Cas12b assay. (A) Fluorescence slope values across serial ten-fold dilutions of V. longisporum template DNA, ranging from 10^5 to 10^0 copies μL^{-1}. Data represent mean ± SD. * denotes statistically significant difference. (B) Real-time fluorescence kinetic curves for serially diluted template and no-template control (NTC). (C) Visual colorimetric readout in reaction tubes. Labels 1E5-1 to 1E0-2 correspond to template concentrations of 10^5-10^0 copies μL^{-1}, with two technical replicates for each concentration. NTC-1 and NTC-2 represent no-template control replicates. Positive samples exhibit green fluorescence, whereas negative controls remain colorless.

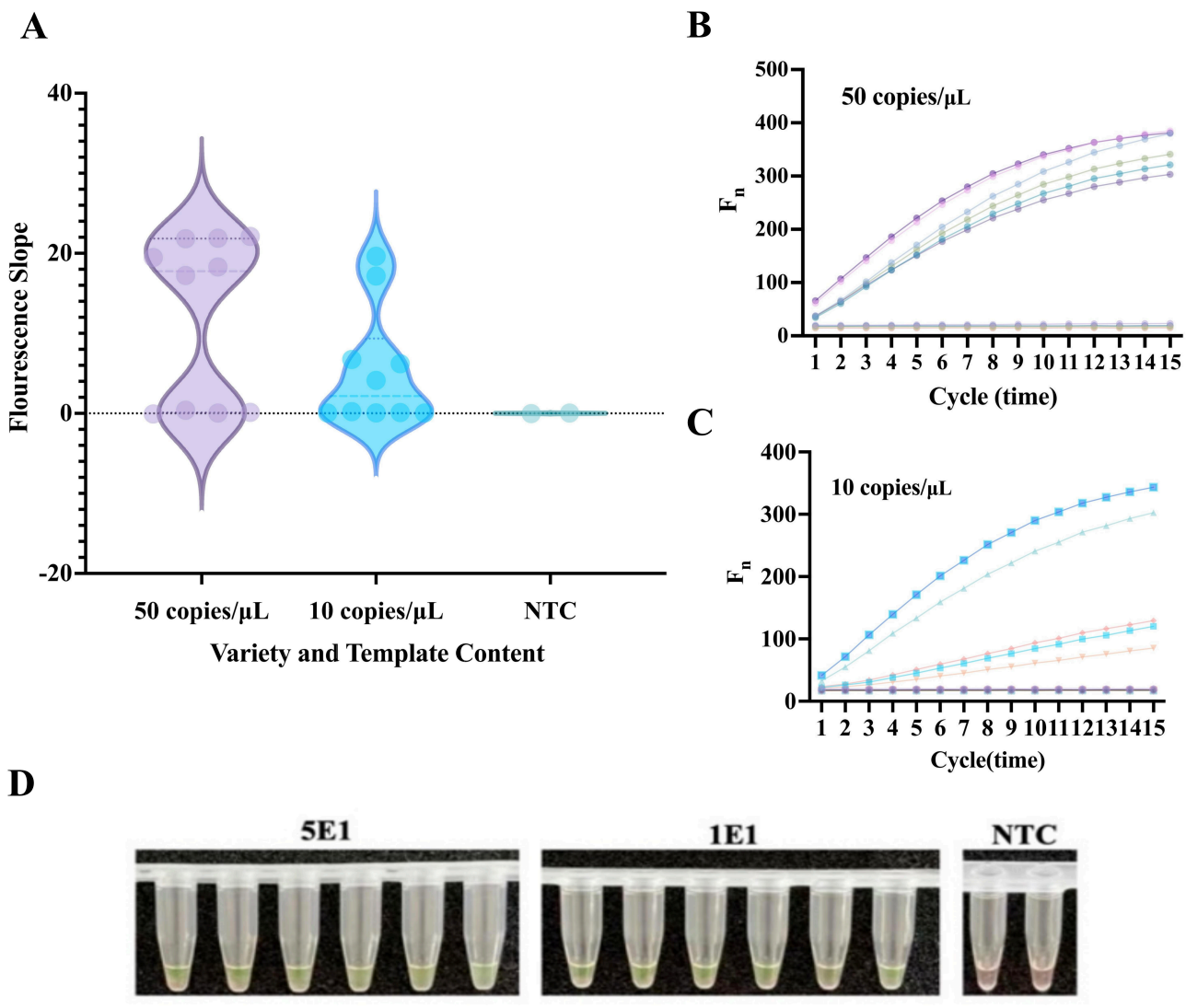


Figure 6

Performance of the one-tube visual RPA-CRISPR/Cas12b detection assay for *V. longisporum*.

(A) Violin plot showing fluorescence-slope values for template concentrations of 50 copies/μL, 10 copies/μL and the non-template control (NTC). Individual replicates are overlaid as scatter points.

(B-C) Real-time fluorescence kinetics of the assay using 50 copies/μL (B) and 10 copies/μL (C) template.

(D) Blue-light visual readout of reaction tubes. 5E1 = 50 copies/μL, 1E1 = 10 copies/μL; NTC, non-template control.

Supplementary Files

This is a list of supplementary files associated with this preprint. Click to download.

- Additionalfile1.pdf